Egyptian Journal of Chemistry

http://ejchem.journals.ekb.eg/

Effect of Ni Content on the Corrosion Performance of Cu-10Al-Ni Ternary Alloys in Neutral Sulfate Solutions

H. Nady[a,b]*, M. M. El-Rabiei[b]*, N. H. Helal[b], W. A. Badawy[c]

[a] *Chemistry Department, College of Sciences and Arts, Qurayate, Jouf University, KSA*
[b] *Chemistry Department, Faculty of Science, Fayoum University, Fayoum-Egypt*
[c] *Chemistry Department, Faculty of Science, Cairo University, 12 613 Giza- Egypt*

Abstract

The present work focuses on the effect of Ni content (0, 5, 10, and 30 %) on the corrosion behavior of Cu-10Al-xNi ternary alloys in Na_2SO_4 solutions. The electrochemical properties were investigated in Na_2SO_4 solutions by polarization measurements, cyclic voltammetry and electrochemical impedance spectroscopy, EIS, techniques. Surface examination and morphological studies were employed. The results show that the addition of Ni to Cu-Al alloys increases the corrosion resistance. Also, the increase in the Ni content improves the corrosion resistance of the Cu-Al-Ni ternary alloys due to formation of a stable passive film. The mechanism of the corrosion process and the barrier film formation was discussed. The experimental EIS data were fitted to the theoretical data according to the suggested model. The incorporation of Ni in the cuprous oxide (Cu_2O) barrier film leads to its stabilization. An equivalent circuit model for the electrode/electrolyte interface under different conditions was proposed. For industrial applications, the results lead to the recommendation of the Cu-10Al-30Ni alloy for applications in the production of Na_2SO_4.

Keywords: Cu-Al-Ni alloy; Corrosion; Cyclic voltammetry; Impedance; Passivation

1. Introduction

Copper and its alloys have many industrial applications because of their good physical properties, excellent machinability, high thermal and electrical conductivity, and good corrosion resistance properties [1-3]. The addition of Al to Cu-based alloys increases its corrosion resistance while the presence of Ni is essential in the passivation of Cu-Ni alloys because of its incorporation in the Cu_2O film, which is formed on the corroded surface of the alloy. There is a wide range of materials which exhibit the shape memory effect, but only those alloys are commercially attractive which show a substantial amount of strain recovery and generate significant force due to shape change [4]. The electrochemical corrosion of Cu-Ni alloys has been extensively examined under different experimental conditions using various techniques [5–9]. It was found that the

_____

increase of Ni-content improves the stability of the Cu-Ni alloy at high NaCl concentrations (> 0.5M) [10]. The corrosion behavior of Cu-Al-Ni alloy in Na_2SO_4 solutions was found to be due to the dissolution of Cu to Cu^{2+} and the passivity was due to the formation of a $Ni(OH)_2$ layer [11, 12]. In alkaline Na_2SO_4 solutions, the corrosion resistance of the Cu-Ni alloys increases with the increase of the nickel content. A critical SO_4^{--} ions concentration was reported, below which the stability decreases and protective film breakdown takes place [9, 13-15]. In this paper, focus has been made on the role of Ni content on the corrosion resistance of the Cu-10Al-xNi ternary alloys with constant Al ratio of 10% in neutral Na_2SO_4 solutions, aiming at the categorization of these alloys according to their stability in this simulated marine solution and to recommend the use of the alloys in such medium, especially for the industrial production of Na_2SO_4. In this respect, different electrochemical techniques, e.g., polarization techniques and EIS were used. The presence of Ni and Al in the protective film structure and surface composition was investigated by EDX analysis and the surface morphology was examined by SEM.

2. Experimental details

The mass spectrometric analysis of the electrodes used in this work is presented in **Table 1**. The investigated electrodes were made from commercial grade Cu-Al-Ni rods, mounted into glass tubes by two-component epoxy resin leaving a surface area of 0.2 cm^2 to contact the corrosive solution. The electrochemical measurements and corrosion behavior tests were carried out in a standard conversional three-electrode all-glass cell with saturated calomel electrode, SCE, and Pt foil serving as the reference and counter electrodes respectively. At the beginning of the tests, the open circuit potential was measured. Before each experiment, the working electrode was polished mechanically using successive grades emery papers up to 2000 grit. The electrochemical measurements were carried out in a naturally aerated Na_2SO_4 solution of pH 7. The polarization experiments and electrochemical impedance spectroscopic investigations, EIS, were performed using a Voltalab PGZ 100 "*All-in-one*" potentiostate/Galvanostate system. All The

polarization experiments were carried out using a scan rate of 10 mV s^{-1}. Prior to the potentiodynamic polarization, the working electrodes were immersed in the solutions for 1 hr for stabilization of the OCP. All cyclic voltammetry measurements were carried out using a scan rate of 10 mV s^{-1}. The total impedance, Z, and phase shift, θ, were recorded in the frequency domain 0.1 to 10^5 Hz. The superimposed ac-signal was 10 mV peak to peak amplitude. The surface morphology and the passive film analysis were performed by SEM/EDAX (model ISPECT S 2006, FEI Company, Holland). To achieve reproducibility, each experiment was carried out at least twice. Details of experimental procedures are as described elsewhere [15-17].

Table 1:

Mass spectrometric analysis for the different electrode materials in mass%

Sample	Cu	Al	Ni	Zn	Mn	Sn	Fe	Si	Mg	Ti
Cu-10Al	88.58	10.19	0.027	0.12	0.01	0.2	0.69	0.037	0.004	0.001
Cu-Al-05Ni	81.16	11.15	4.98	0.11	0.02	0.14	2.22	0.21	0.01	-----
Cu-Al-10Ni	76.00	11.28	9.95	0.10	0.02	0.14	2.26	0.24	0.01	------
Cu-Al-30Ni	60.02	9.32	29.17	0.08	0.01	0.13	1.10	0.16	0.01	-----

3. Results and discussion

3.1. Open-circuit potential measurements, OCP.

OCP of Cu, Ni and Cu-Al-Ni ternary alloys with different Ni contents (0, 5, 10 and 30 mass% Ni) were traced over 1h in the 0.2 M SO_4^{2-} solution. Results of OCP were measured against a SCE are shown in **Fig. 1a**. The OCP of Cu-Al-Ni alloys with different Ni content (0-30%) shift towards positive values and lie in the range of Cu. The steady-state potential, E_{ss}, for all investigated electrodes was reached within 30 min from electrode immersion in the test electrolyte and varied in narrow range. **Fig. 1b** shows the variations of the OCP with time for Cu-10Al-30Ni alloy in neutral solution containing different SO_4^{2-} ions concentrations. As can be seen the OCP gradually shifts towards less negative values until it reaches a relatively steady value, E_{ss}, after

about 40 min from immersion in Na_2SO_4 solution. This behavior indicates that a passivation process occurs at the electrode/electrolyte interface. Visual observation of the surface of the electrode during immersion tests reveals continuous decrease in the rate of H_2 gas evolution on Cu-Al-Ni surface with immersion time, suggesting a decrease in its rate of corrosion. This is likely attributed to deposition of corrosion products on the alloy surface as a result of interaction between the metal surface and SO_4^{2-} anions in solution. As the SO_4^{2-} ions concentration increases the E_{ss} for Cu-10Al-30Ni alloy shifts towards more positive values up to 0.2 M then gets more negative shift, which was attributed to the selective leaching of the active components from the alloy surface [18]. This behavior indicates that the corrosion process of Cu-Al-30Ni alloy in Na_2SO_4 solution depend on the properties of the corrosion film formed on the alloy surface as a function of the SO_4^{2-} ion concentration.
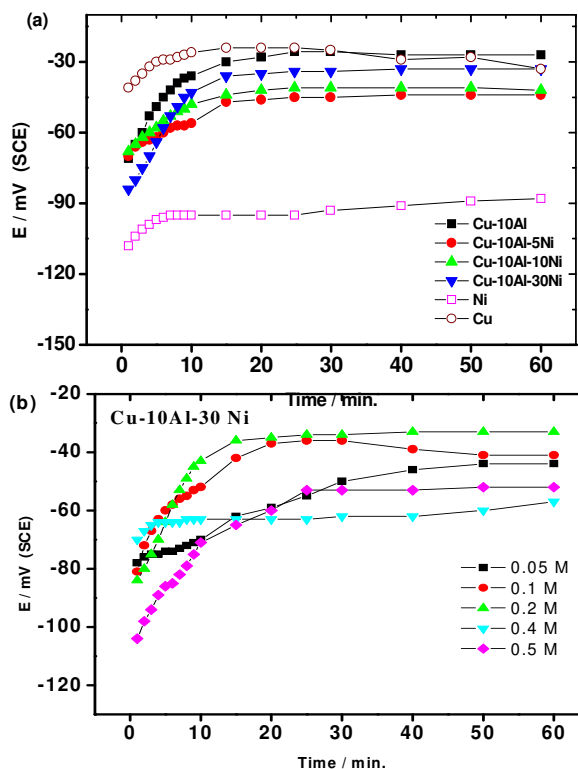

Fig. 1- (a) Variation of the OCP of Cu, Ni and Cu-Al-Ni alloys in 0.2 M Na_2SO_4. (**b**) Variation of the OCP of Cu-10Al-30Ni alloy with time in neutral Na_2SO_4 solution of different concentrations.

3.2. Cyclic voltammetric investigations, CV.

CVs for Cu, Ni, and different Cu-Al-Ni alloys were recorded at a scan rate of 10 mV s^{-1} in 0.2 M Na_2SO_4 solution of pH 7. The CV of Ni in Na_2SO_4 solution at 25 ^{o}C is shown in **Fig. 2a**. The potential scan was started at -800 mV, where a significant cathodic current is observed due to the generation of H_2 gas. The cathodic current density rapidly diminishes as the E is made less negative. There is then an unclear active region for dissolution of Ni, in which the current density increases slightly with increasing the potential. On the anodic part, oxidation started at about -420 mV followed by a small anodic dissolution current. It was reported that the predominant soluble Ni species in neutral solutions were either $Ni(OH)^+_{(aq)}$ or $Ni^{2+}_{(aq)}$ ions [19,

20]. The Ni dissolution has been reported to be dependent on the solution pH, which suggests a contribution of OH^- to the active metal dissolution process [20-22]. The dissolution reactions of Ni can be represented as the following [20, 21]: $Ni + OH^- = Ni(OH)_{ads} + e^-$, $Ni + H_2O = Ni(OH)_{ads} + H^+ + e^-$, $Ni(OH)_{ads} = Ni(OH)^+_{aq} + e^-$, $Ni + SO_4^{-2} = NiSO_4 + 2e^-$. It is a reasonable assumption to hold the same primary step ($Ni + OH^- = Ni(OH)_{ads} + e^-$ and $Ni + H_2O = Ni(OH)_{ads} + H^+ + e^-$) responsible for passivation: $Ni(OH)_{ads} + OH^- = Ni(OH)_2 + e^-$, $Ni(OH)_{ads} + H_2O = Ni(OH)_2 + H^+ + e^-$ and $Ni(OH)_2 = NiO + H_2O$. The reverse potential scan does not show a cathodic peak corresponding to the reduction of the passive film. This can be attributed to either the high stability of the passive film or the overlap of

_____

the reduction of dissolved oxygen and passive film just preceding the potential range of the H_2 generation reaction [23]. The CV for Cu in 0.2 M Na_2SO_4 solution is presented in **Fig. 2b**. The cathodic current density decreases as the potential is made less negative. There is then a transition region before the active dissolution of Cu commences. In this region, the current density stabilizes with increasing potential. This plateau is most probably due to the formation of $Cu(SO_4)^{2-}_{ads}$, and/or $Cu(OH)^-_{ads}$ adsorbed species at the metal surface [24, 25] according to the reactions: $Cu + SO_4^{-2} = Cu(SO_4)^-_{ads}$, $Cu + OH^- = Cu(OH)^-_{ads}$ and $Cu + H_2O = Cu(OH)^-_{ads} + H^+$. Usually, the adsorption of anions (such as sulfate ions) on the metal surface may promote dissolution or passivation with increasing potential [26]. Several studies have confirmed the adsorption of SO_4^{-2} ions on Cu electrode in acid and neutral electrolytes [25, 27]. The $Cu(SO_4)^{-2}_{ads}$ and/or $Cu(OH)^-_{ads}$ species represent an adsorbed intermediate for active metal dissolution. In the anodic region, Cu goes into solution as Cu^+ ions [24, 28], the current density is continuously increasing with potential. The increase in anodic current can be attributed to dissolution process of the adsorbed layer which can be described as follows: $Cu(OH)^-_{ads} + OH^- = Cu(OH)_2^-{}_{(aq)} + e^-$, $2 Cu(SO_4)^{-2}_{ads} = Cu_2(SO_4)_{(aq)} + SO_4^{-2} + e^-$. The CVs for Cu-10Al, Cu-10Al-5Ni, Cu-10Al-10Ni, and Cu-10Al-30Ni in 0.2 M Na_2SO_4 solution are presented in **Fig. 2(c-f)**. The shapes of the cyclic voltammograms of the alloys resemble that of pure Cu more than that of pure Ni. This means that the kinetic process is controlled by the Cu dissolution. This confirms the data obtained by OCP. **Fig. 3** displays the influence of different SO_4^{-2} ion concentrations on the CV of Cu-Al-5Ni alloy. It can be observed that the same behavior took place when the concentration of SO_4^{-2} ions increases in case Cu-

Al, Cu-Al-10Ni and Cu-Al-30Ni alloys. The same peaks appeared in this range of SO_4^{-2} ion concentration and a limited change in the position of the peaks observed. This means that the mechanism of the corrosion process does not change.
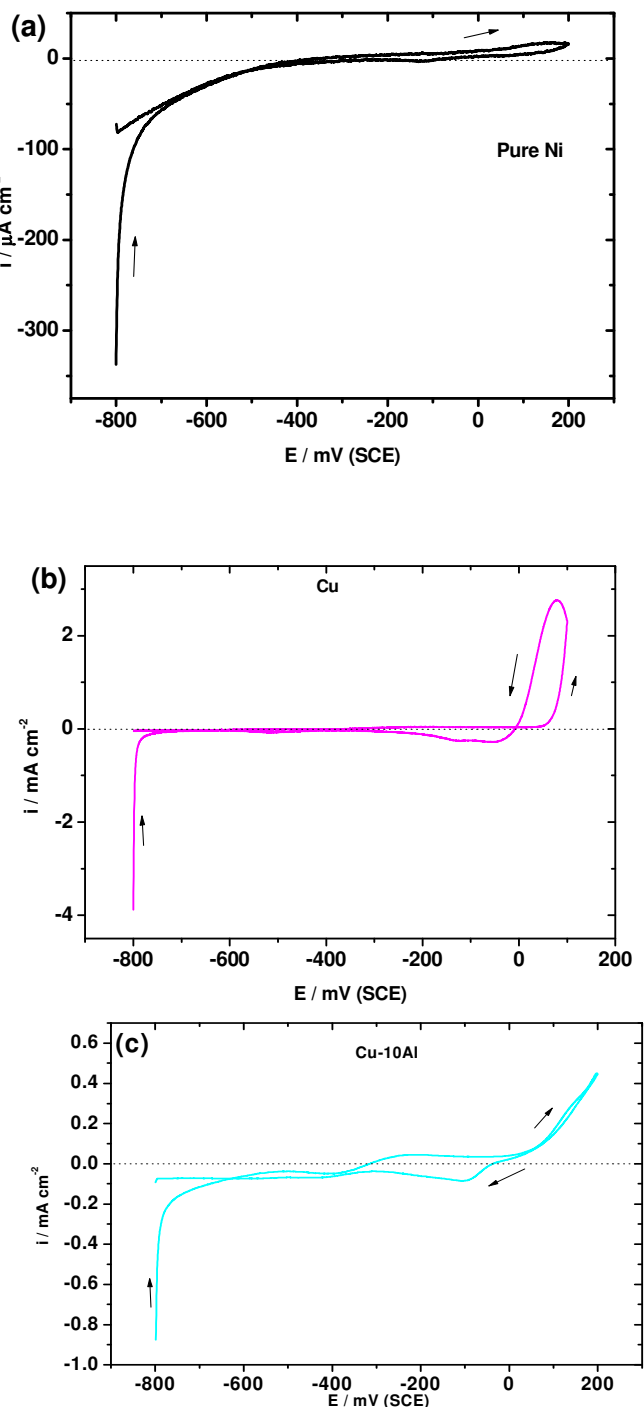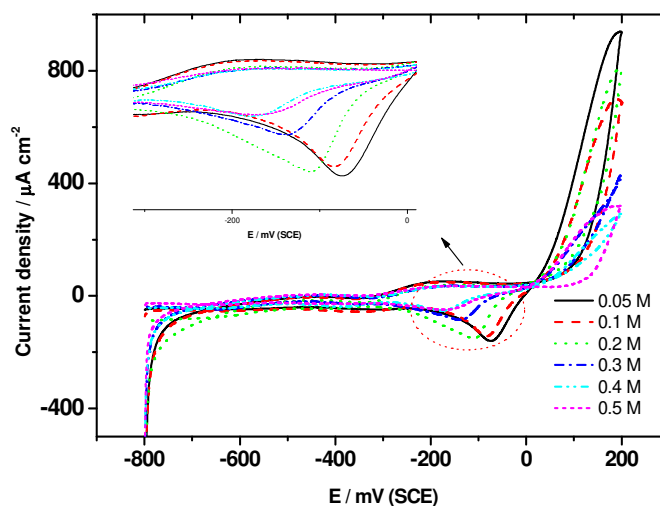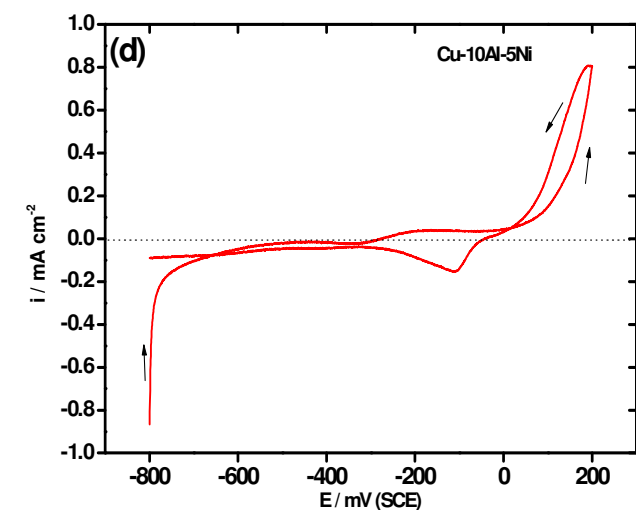
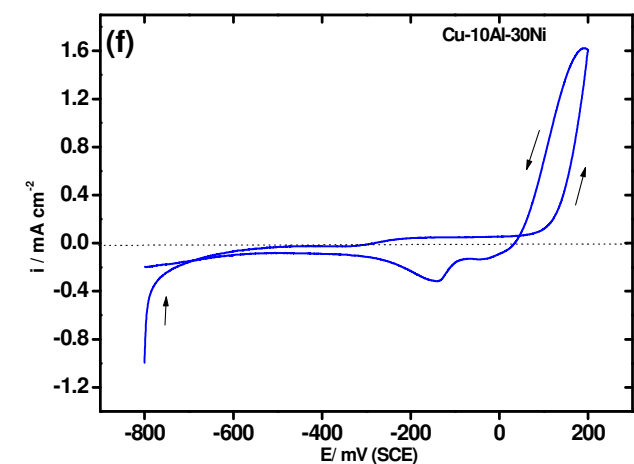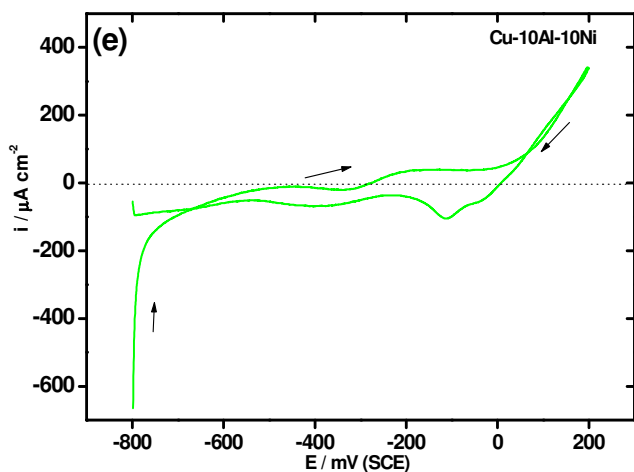**Fig. 3-** CV of Cu-10Al-5Ni alloy in Na$_2$SO$_4$ solution of different concentrations.
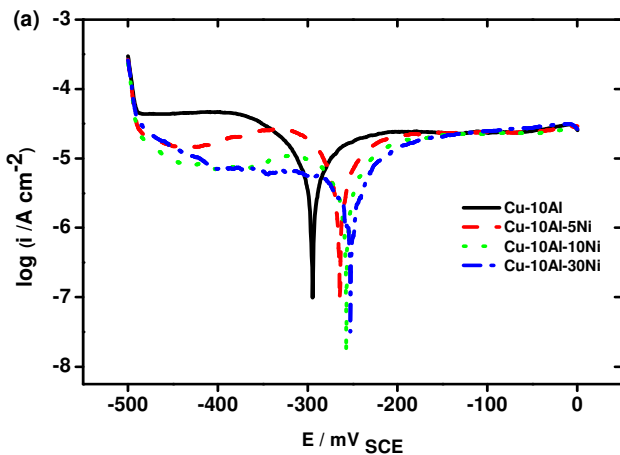
3.3 The corrosion rates of Cu-Al-Ni alloys

The corrosion behavior of Cu-Al-Ni alloys with various Ni contents was investigated in Na$_2$SO$_4$ solution. The potentiodynamic polarization curves of the different alloys after immersion in 0.2 M Na$_2$SO$_4$ solution are presented in **Fig. 4a**. The values of the corrosion parameters, corrosion current density, i_{corr}, Tafel slopes, β_a & βc and corrosion potential, E_{corr}, were calculated and presented in **Table 2**. The relation between the corrosion current density, i_{corr}, and Ni content are presented in **Fig 4b**. It was found that, the corrosion rate decreases with addition of Ni to Cu-Al alloy, also decrease with the increasing Ni content in the Cu-Al-Ni alloys. This result can be explained on the basis of the dissolution of Ni with the formation of Ni^{2+} ions followed by the formation of a protective film of Ni(OH)$_2$ or NiO. After reaching the steady state, the ability of the barrier film to impart passivity depends on the amount of NiO in the protective layer which in turn is dependent on the Ni content. The corrosion behavior of the Cu-Al-Ni ternary alloys is controlled by the passivating properties of Ni and hence the corrosion current density decreases as the Ni content increases. The effect of SO$_4^{-2}$ ions concentration on the corrosion rates of Cu-Al-Ni ternary alloys was investigated using potentiodynamic polarization technique. The potentiodynamic polarization curves of Cu-10Al and Cu-10Al-30Ni alloys at different concentration of Na$_2$SO$_4$ are presented in **Figs. 5a and b**. The corrosion parameters values, i_{corr}, βa & βc and E_{corr}, were calculated and presented in **Table 3**. For different Cu-10Al-$_x$Ni alloys, the i_{corr} decreases with the increase in Na$_2$SO$_4$ concentration as presented in

Fig. 2- CVs of Ni (a), Cu (b) and Cu-Al-Ni alloys (c-f) in 0.2 M Na$_2$SO$_4$ solutions.

Fig. 5c. The corrosion resistance of the Cu-Al-Ni ternary alloys is attributed to a spontaneously formed protective film consisting mainly of barrier Cu_2O layer, which is in a contact with the electrolyte through a porous outer layer of Cu(II) hydroxide/oxide [29, 30]. From the polarization measurements, the i_{corr} values are generally decreased with increasing the Ni content which means that the composition of the barrier layer formed on Cu and Cu-Al-Ni ternary alloys is not identical. In the point defect model (PDM) [31] and the solute vacancy interaction model (SVIM) [32], the Cu_2O film is regarded as a p-type semiconductor, and therefore the mobile cation vacancies (V_{Cu}-(ox)$_{red}$ are the main charge carriers ($Cu_{Cu}(ox) \rightarrow Cu^+(aq) + V_{Cu}-(ox)$)). Ni from the Cu-Al-Ni alloy are incorporated into the crystal lattice of Cu_2O layer, where Ni^{2+} cations interact with mobile negatively charged cation vacancies and form neutral complexes according to [33-35]: $Ni_{Ni}(m) + 2V_{Cu}-(oX) \rightarrow [Ni_{Cu}(V_{Cu})_2] + 2e^-$. The $[Ni_{Cu}(V_{Cu})_2]$ formation leads to a decrease in the ionic conductivity and increase of the electronic conductivity of the protective layer and the corrosion resistance thus increased [36, 37]. In the case of the protective film formed on Cu-Al-Ni ternary alloys, the Ni incorporation process from the metal/oxide interface plays an important role. It seems reasonable to assume that barrier Cu_2O layer doped with Ni should exhibit a higher corrosion resistance compared to a simple Cu_2O layer [38].
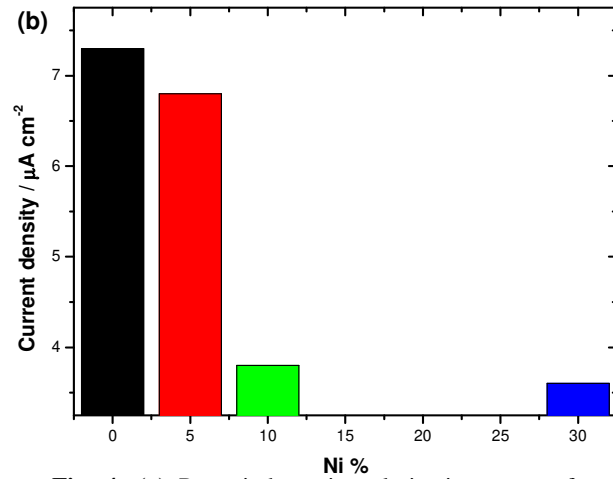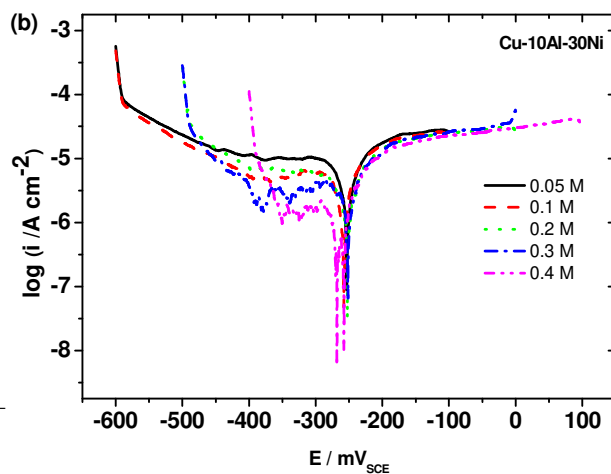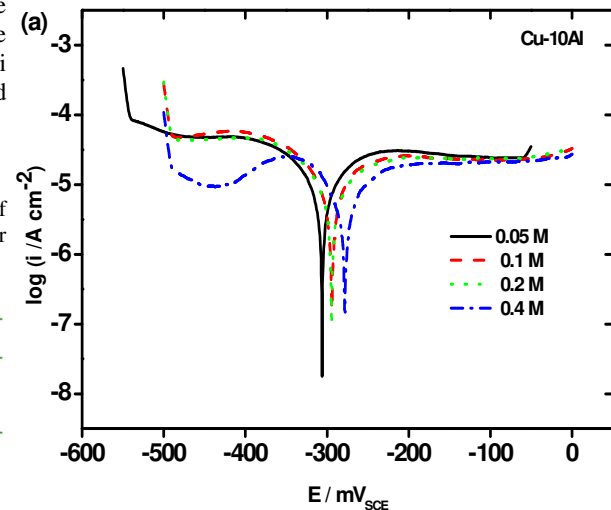

Fig. 4- **(a)** Potentiodynamic polarization curves for the Cu-Al-Ni alloys in 0.2M Na_2SO_4 solution. **(b)** The corrosion current density of the investigated alloys as a function of the Ni content.

Table 2: Polarization parameters and rates of corrosion of the different Cu-Al-Ni alloys in 0.2 M Na_2SO_4, pH 7.0 after electrode immersion at 25 $^\circ$C.

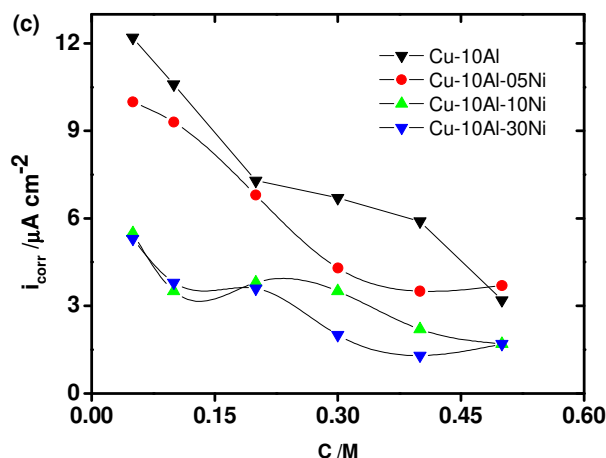| Alloys	E_{corr} / mV	i_{corr} / $\mu A\ cm^{-2}$	β_a / mV	β_c / mV	Corr. Rate/$\mu m\ Y^{-1}$
Cu-10Al	-290.6	7.3	93.6	-84.3	84.7
Cu-10Al- 05Ni	-259.6	6.8	111.9	-96.1	80.0
Cu-10Al -10Ni	-255.4	3.8	69.0	-108.1	44.3
Cu-10Al -30Ni	-246.9	3.6	95.5	-122.6	42.0

Fig. 5- Potentiodynamic polarization curves for Cu-10Al (a) and Cu-10Al-30Ni (b) alloys in different concentration of SO_4^{-2} ions. **(c)** The corrosion current density of the different alloys as a function of SO_4^{-2} ions concentration.

Table 3: Polarization parameters and rates of corrosion of the different Cu-Al-Ni alloys in different concentration of Na_2SO_4 solution of pH 7.0 after electrode immersion at 25 ˚C.

	SO_4^- / M	E_{corr} / mV	i_{corr} / $\mu A\ cm^{-2}$	β_a / mV	β_c / mV	Corr. Rate / $\mu m\ y^{-1}$
Cu-10Al	0.05	-304.1	12.2	130.3	-141.4	141.8
	0.1	-292.6	10.6	164.0	-104.3	122.9
	0.2	-290.6	7.3	93.6	-84.3	84.7
	0.3	-289.9	6.7	100.3	-96.5	77.5
	0.4	-275.2	5.9	108.6	-108.5	69.2
Cu-10Al-5Ni	0.05	-259.9	10.0	201.1	-113.5	116.3
	0.1	-257.3	9.3	197.9	-127.7	108.1
	0.2	-259.6	6.8	111.9	-96.1	80.0
	0.3	-246.7	4.3	103.3	-61.6	50.3
	0.4	-329.0	3.5	64.0	-73.5	40.7
Cu-10Al-30Ni	0.05	-249.2	5.3	114.2	-80.4	62.2
	0.1	-255.2	3.8	78.3	-224.3	44.4
	0.2	-246.9	3.6	95.5	-122.6	42.0
	0.3	-249.5	2.0	65.3	-109.8	33.4
	0.4	-269.2	1.3	74.7	-40.0	14.6

3.3.4 EIS measurements,

The impedance spectra of Cu-10Al-30Ni alloy in 0.2 M Na_2SO_4 solution after different immersion times are illustrated in **Fig. 6**. The Bode plot (*cf.* Fig. 6a) showed that the total impedance magnitudes of the alloy samples at the lowest frequency increased with immersion time, indicative of the increase in the corrosion resistance due to the formation of a protective oxide film on the alloy surface. From the respective phase angle Bode plots, two peak maxima were distinguished. The peak angles appearing in the low frequency range were attributed to the protective oxide film. The maximum peak angles at the high frequency range may derive from the electrical double layer. The experimental data fitted to the equivalent circuit model of Fig. 6a (inset). In the proposed equivalent circuit model, Rs and Rct represent the solution and the charge transfer resistances, respectively. Both resistances are in parallel to a capacitor that characterizes the double-layer capacity, Cdl. Also, an additional resistor, Rf, and capacitor, Cf, were introduced to consider the formed surface film. The equivalent circuit parameters for the different Cu-Al-Ni alloys at different intervals of electrode immersion in Na_2SO_4 solution are presented in **Table 4**. The increase of the impedance values is due to the progressive formation of the protective layer on the surface of alloys. The passive film resistance, R_{pf}, for the Cu-10Al-30Ni alloy increases with the increase in time of immersion, while the passive film thickness, $1/C_{pf}$, increases up to 90 min then decrease (*cf.* Fig. 6b).

The influence of Na_2SO_4 ion concentration on the corrosion process of the Cu-10Al-30Ni alloy was investigated using the EIS measurements. The experimental Bode plots obtained with the Cu-10Al-30Ni alloy after 1h of electrode immersion in solutions with different concentrations of SO_4^{-2} ions (0.05-0.5 M) are presented in **Fig. 7a**. Using the equivalent circuit model shown in Fig. 6a (*inset*), the calculated parameters for Cu-10Al-30Ni alloy after electrode immersion in solutions with different concentration of SO_4^{-2} ions are presented in **Table 5**. **Fig. 7b** shows the variations of the R_{pf} and the $1/C_{pf}$ with Na_2SO_4 concentration for Cu-10Al-30Ni alloy. It is clear that the addition of up to 0.1 M Na_2SO_4 leads to a decrease in R_{pf} and $1/C_{pf}$ due to dissolution of the adsorbed species and formation of the soluble Cu_2SO_{4aq} [13]. Above this concentration, R_{pf} and $1/C_{pf}$ increase due to formation of adsorbed species $\{Cu(SO_4)_{ads}^-\}$. The accumulation of higher sulfate ions concentration leads to the stabilization of the adsorbed layer and then an increase in both R_{pf} and $1/C_{pf}$ could be recorded.
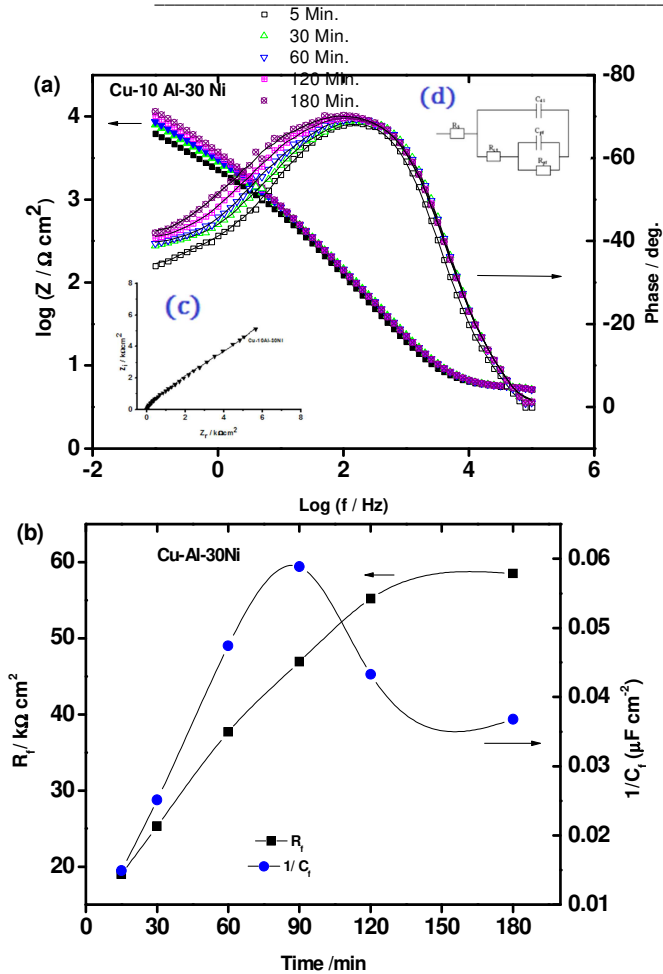
Fig. 6- (a) Bode plots of Cu-10Al-30Ni alloy after different times of immersion in 0.2M SO4-2 solution. Fig. 6a inset (c) Experimental Nyquist plots recorded in 0.2 M SO4-2 solutions for Cu-10Al-30Ni alloy. The solid lines represent the fitted data according to the equivalent circuit model of (d) inset. Fig. 6a inset (d) Equivalent circuit model used in the impedance data fitting (Rs = solution resistance, Rp = charge-transfer resistance, Cdl = double layer capacitance, Rpf =passive film resistance, and Cpf =passive film capacitance). (b) The barrier film resistance, Rpf, and relative film thickness, 1/Cpf, formed on the Cu-Al-30Ni alloy surface in 0.2 M SO4-2 neutral solutions as a function of the time immersion.
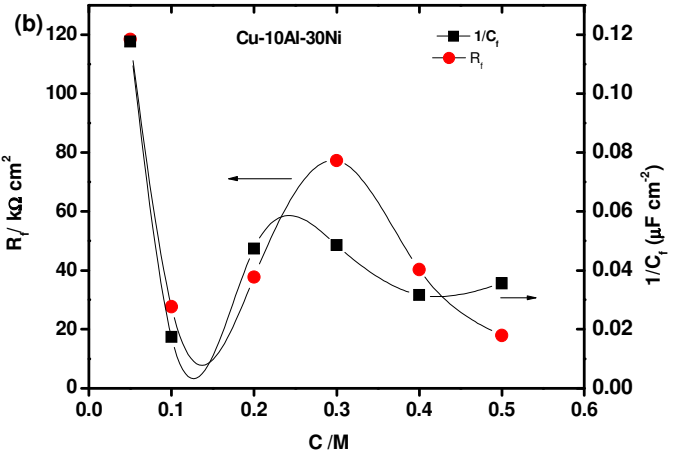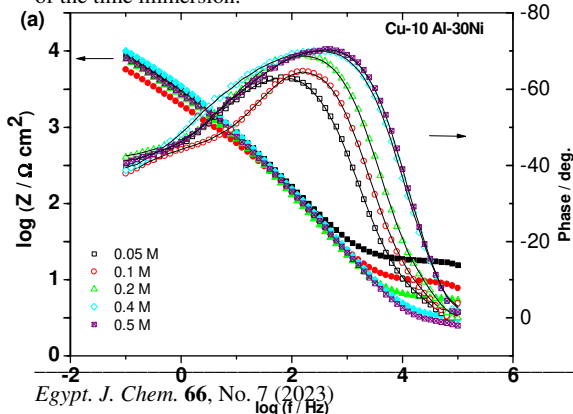

Fig.7- (a) Bode plots of Cu-10Al-30Ni alloy after immersion in neutral solutions containing different SO_4^{-2} ion concentrations. (b) Variation of passive film resistance, R_{pf}, and relative passive layer thickness, $1/C_{pf}$ of the Cu-10Al-30Ni alloy as a function of SO_4^{-2} ions concentration.

3.3.5. SEM/EDAX analysis

The surface morphology of the different alloys after immersion in Na_2SO_4 solution was investigated by SEM. Figures 8 and 9 shows SEM/EDX images of the Cu-10Al (8a and 9a) and Cu-10Al-30Ni (8b and 9b) alloys before and after immersion in Na_2SO_4 solution, where the corrosion sites are clearly observed. Alloys with 30% Ni did not show any flawed regions, which means that the addition of Ni improves the stability of the alloy as was demonstrated by the polarization and EIS investigations (cf. Fig. 9b). The surface of the Cu-10Al and Cu-10Al-30Ni alloy was subjected to EDAX analysis to record the different constituents of the barrier layer (*cf.* Figs. 8 and 9). It is clear that the constituent elements of the alloys are present in the passive film by almost the same ratio as the alloy itself. This means that the elements, Al, Cu, and Ni are participating in the passivation process.
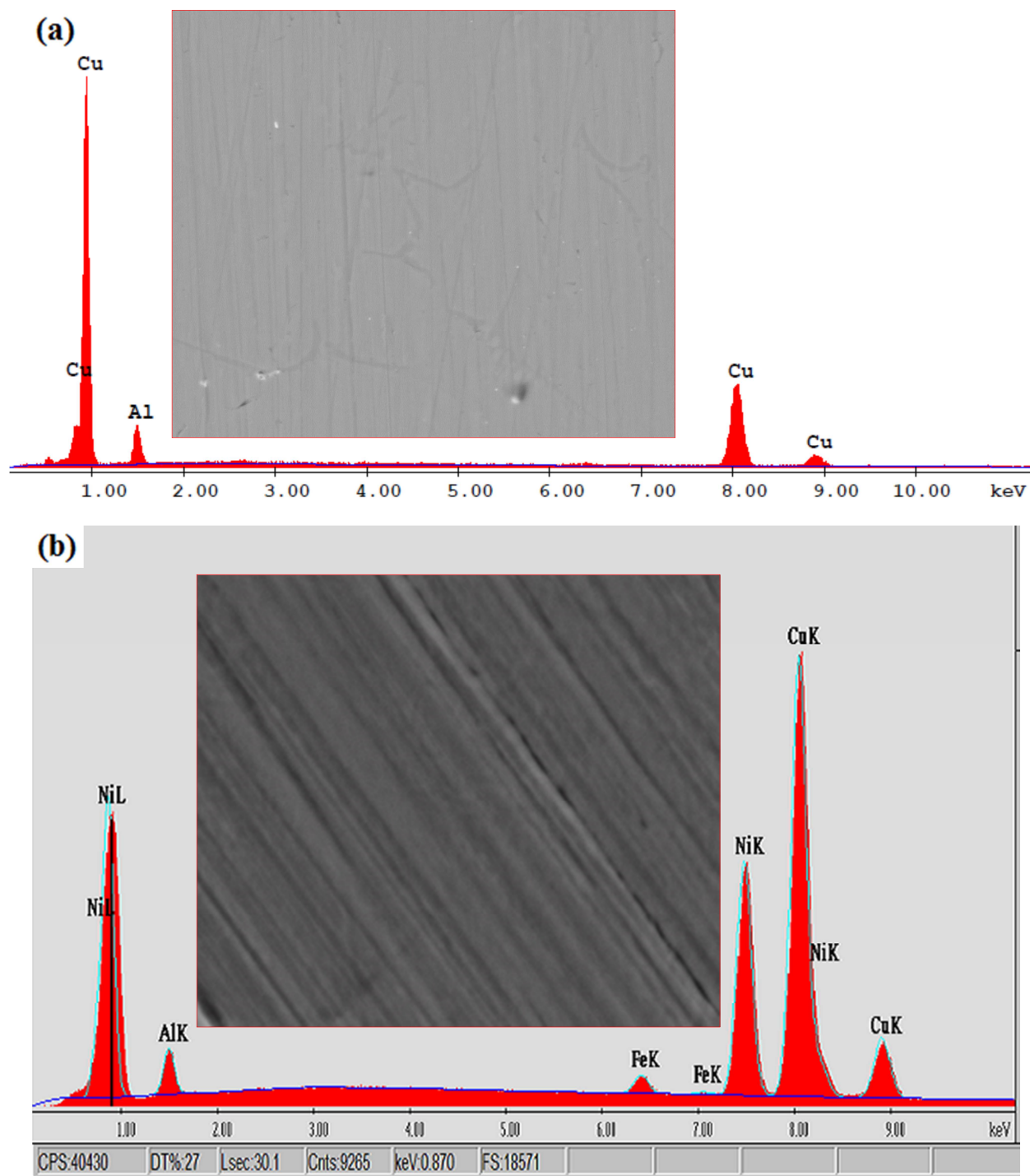
Fig.8- SEM and EDAX analysis of (a) Cu-Al and (b) Cu-Al-30Ni alloy before electrochemical testing.
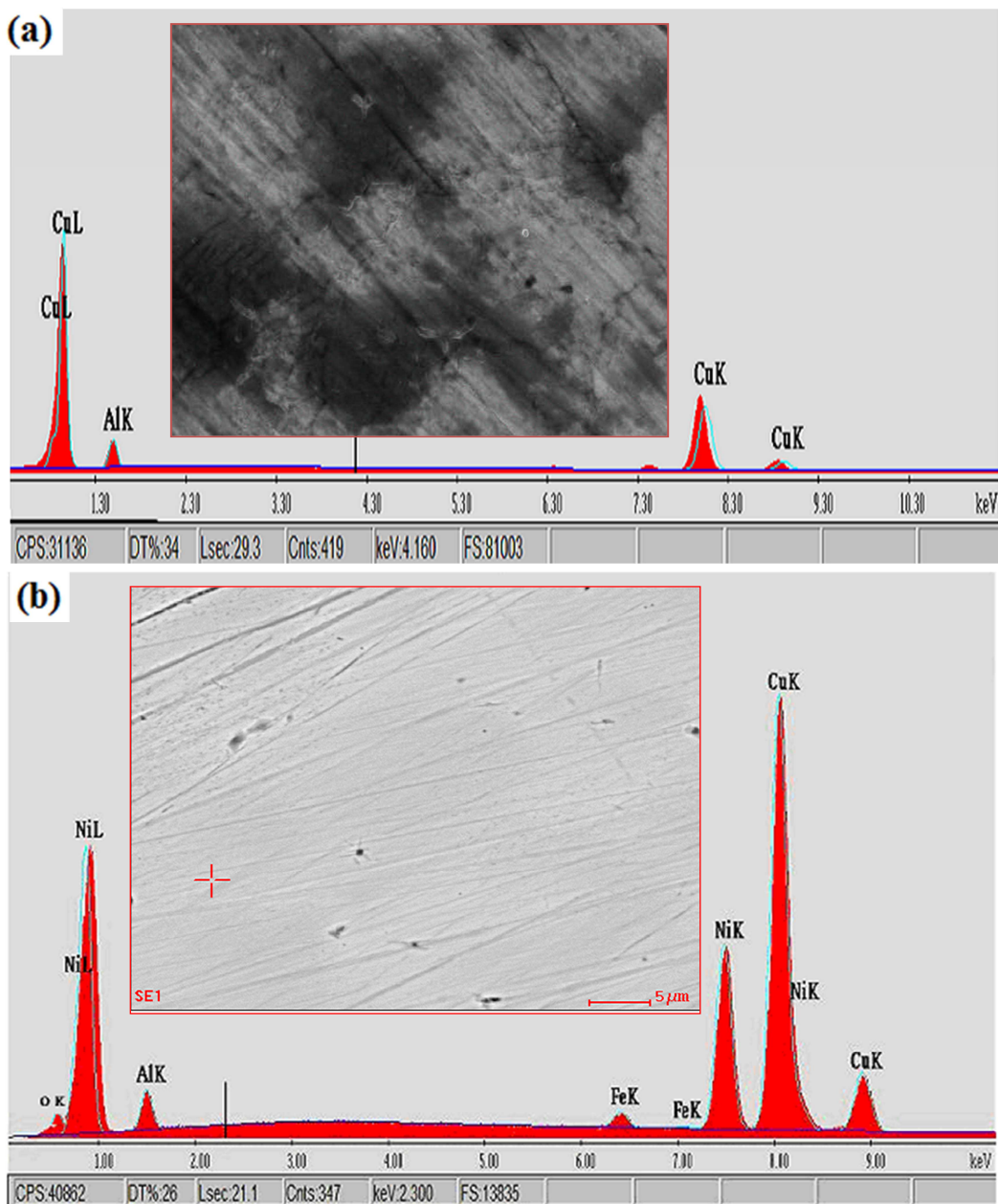
Fig. 9- SEM/EDX analysis of Cu-Al and Cu-10Al-30Ni alloy after immersion in neutral solution 0.5 M SO_4^{-2} solutions and 25 °C

4. Conclusion

The stability of the Cu-10Al-$_x$Ni ternary alloys in SO_4^{2-} solutions depends on the Ni content. The corrosion rate of Cu-Al-Ni alloys decrease with the increase in the concentration of sulfate ions. Alloys with $\geq$ 30% Ni show limited corrosion rate. The passive film that protects the alloys against corrosion is affected by the Na_2SO_4 concentration. The passive layer formed on the alloy surface consists of a continuous porous layer on the top of a thin barrier film.

_____

5. Conflicts of interest: On behalf of all authors, I confirm that this manuscript has no conflict of interest.

6. Acknowledgments

7. References

[1] E.A. Ashour, B.G. Ateya, Electrochim. Acta, 42 (1997) 243.

[2] X.Z. Zhou, C.P. Deng, Y.C. Su, J. Alloy Compd. 491 (2010) 92.

[3] H. Nady, M. M. El-Rabiei, W. A. Badawy & M. Samy, . J Bio Tribo Corros 4(2018) 1-8

[4] Ashish Agrawal, Ravindra KumarDube, Journal of Alloys and Compounds
 750 (2018) 235-247.

[5] K.M. Ismail, A.M. Fathi,W.A. Badawy, Corros. Sci. 48 (2006) 1912.

[6] W.A. Badawy, K.M. Ismail, A.M. Fathi, Electrochim. Acta 50 (2005) 4182

[7] Ghalia Asaad Gaber; Walaa A. Hussein; Amal S. I. Ahmed, Egypt. J. Chem. 63(2020) 1527.

[8] Hashem M. Nady, Mohammed M. El-Rabiei1 and Waheed A. Badawy, Chemical and Process Engineering Research, 20 (2014) 35

[9]. H. Nady, M. M. El-Rabiei, G. M. Abd El-Hafez, J Bio Tribo Corros 2(2016) 28

[10] I. Milosev, M. Metikos-Hukovic, Electrochim. Acta 42 (1997) 1537.

[11] H. Nady, M. M. El Rabiei, M. Samy, W. A. Badawy, J Bio Tribo Corros 6 (2020)1-13

[12] R.E. Hummel, R.J. Smith, Corros. Sci. 28 (1988) 279.

[13] K.M. Ismail, A.M. Fathi,W.A. Badawy, Corros. 60 (2004) 795.

[14] K.M. Ismail, A.M. Fathi, W.A. Badawy, J. Appl. Electrochem. 34 (2004) 823.

[15] W.A.Badawy, R.M.El-Sherif, H.Shehata; Electrochim. Acta 54(2009) 4501.

[16] W.A. Badawy, F.M.Al-Kharafi., A.S.El-Azab. Corros. Sci. 41(1999) 709.

[17] W. A. Badawy, M. El-Rabiee, N. H. Hilal, H. Nady, Electrochimi. Acta 56 (2010) 913.

[18] W.A. Badawy, F.M. Al-Kharafi, A.S. El-Azab, Curr. Top. Electrochem. 6 (1998) 149.

[19] J.A. Ali and J.R. Ambrose, Corros. Sci. 32 (1991) 799.

[20] U. Ebersbach, K. Schwabe, K. Ritter, Electrochim. Acta 12 (1967) 927.

[21] N. Sato and G. Okamoto, in "Comprehensive Treatise of Electrochemistry" Vol. 4, eds. J.O'M. Bockris, B.E. Conway, E. Yeager and R.E. White (New York, NY: Plenum Press, 1981), p. 201.

[22] G. Dagan, M. Tomkiewicz, J. Electrochem. Soc. 139 (1992) 461.

[23] A.E. Bohe, J.R. Vilche, K. Juettner, W.J. Lorenz, W. Paatsch, Electrochim. Acta 34 (1989) 1443.

[24] K.M. Ismail, S.S. El-Egamy and M. Abdelfatah, J. Appl. Electrochem. 31(2001) 663.

[25] L.M. Rice-Jackson, G. Horanyi and A. Wieckowski, Electrochim. Acta, 36 (1991) 753.

[26] V.P. Parkhutik, J.M. Albella, J.M. Martinez-Duart, in: B.E. Conway, J.O'M. Bockris, R.E. White (Eds.), Modern Aspects of Electrochemistry, Number 23, Plenum Press, New York, 1992, p. 330.

[27] S. Magaino, Electrochim. Acta 42 (1997) 377.

[28] A. Jardy, A.L. Lasalle-Molin, M. Keddam and H. Takenouti; Electrochim. Acta, 37(1992) 2195.

[29] R.F. North, M.J. Pryor, Corros. Sci. 10 (1970) 297.

[30] W.A. Badawy, K.M. Ismaila, A.M. Fathi, Electrochim. Acta 50 (2005) 3603.

[31] D.D. Macdonald, J. Electrochem. Soc. 139 (1992) 3434.

[32] D.D. Macdonad, M. Urquidi, J. Electrochem. Soc. 132 (1985) 555.

[33] H. Shih, H.W. Pickering, J. Electrochem. Soc. 134 (1987) 1949.

[34] R.G. Blundy, M.J. Pryor, Corrosion Science 12 (1972) 65.

[35] A.-M. Beccaria, J. Crousier, British Corrosion Journal 24 (1989) 49.

[36] M. Urquidi, D.D. Macdonald, Journal of the Electrochemical Society 132 (1985) 555.

[37] M. Metikoˇs-Hukoviˊ c, R. Babiˊ c, I. ˇSkugor, Z. Grubaˇc, Corrosion Science 53 (2011)347.

[38] J.-D. Kim, S.-I. Pyun, R.A. Oriani, Electrochimica Acta 41 (1996) 57.

_____